SHMS Shielding Design

July 18, 2008

T. H.

Abstract

A specialized shield hut design was developed at Jefferson Lab for the new focusing spectrometer in Hall C to provide shielding of sensitive experimental equipment. It minimizes radiation-induced effects on the performance and reliability of detectors and electronics. The shielding consists of concrete walls to moderate and attenuate particles. Low energy (thermal) neutrons are absorbed in a boron layer. Low energy and 0.5 MeV capture photons are absorbed in lead. The shield wall thicknesses were optimized for the shielding of the detectors and electronics. The shielding for the latter was further enhanced by enclosure in a separate electronics hut. This article provides details about the developement of the conceptual design and its analysis using a Monte Carlo simulation of the setup.

I. INTRODUCTION

The physics program in Hall C at Jefferson Lab after the CEBAF energy upgrade to 12 GeV is focused on measurements of two-body elastic and inelastic reactions. Examples are studies of pion and nucleon form facors at high Q^2, deep inelastic scattering at high Bjorken x, semi-inclusive scattering at high hadron momenta, and polarized and unpolarized scattering on nuclei.

The experiments will be performed using high resolution focusing spectrometers, one of which, the Super High Momentum Spectrometer (SHMS), will be build as part of the upgrade. The design of such a system is concerned with matching the experimental desirability with the technical feasibility.

The experimental program requires detection of charged particles with momenta as high as the incident electron beam (11 GeV/c) for a variety of targets, running at the luminosities of 10^{38} and beam currents currents of up to 90μA. The main concern for experimental equipment under these conditions is radiation damage, and thus one important aspect in the spectrometer design is the protection of its components.

The goal of this report is to describe the design criteria for the shielding designed to protect both detectors and electronics in the SHMS, and to compare these to the performance of existing shielding designs.

The primary particle radiation is created when the CEBAF electron beam strikes the experimental target. The main components are scattered electrons, neutral particles (photons and neutrons), and charged hadrons. The energy spectrum of this radiation depends on the incident beam energy and decreases with energy. It has been shown that the most efficient way to protect

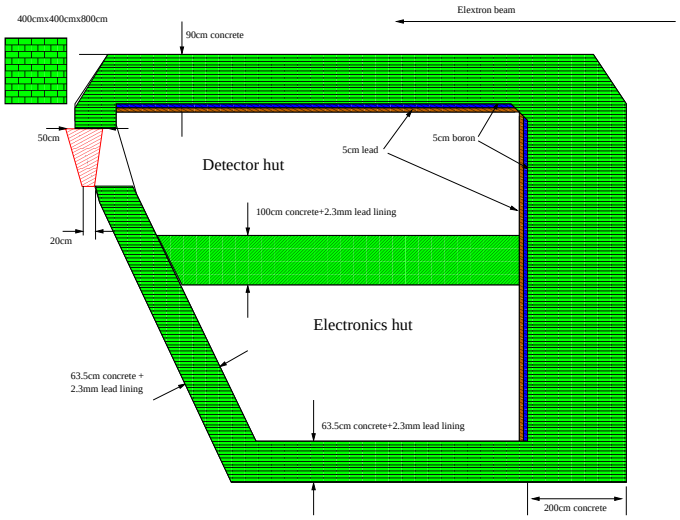

FIG. 1: *Schematic of the proposed SHMS shield house design.*

the experimental equipment from radiation damage is to build a "hut" around it using certain key materials. The type and thickness of the shield hut walls depends on the energy and particle one needs to shield against. However, one may qualitatively expect that the largest amount of shielding material is needed on the side facing the primary source, which in the case of the Hall C focusing spectrometers is the front face. Additional sources of radiation are the beampipe, which extends from the experimental target to the beam dump, and the beam dump area itself. Thus, the faces of the spectrometer exposed to direct sources of radiation are the front, beam side, and the back walls.

Primary and scattered electrons lose a significant amount of energy as they traverse a material by producing a large number of lower energy photons through bremsstrahlung [1] (see Figure 2). It is thus important to consider shielding materials that efficiently stop the latter as well.

Neutral particles have a higher penetration power than charged particles. They are attenuated in intensity as they traverse matter, but do not continously lose energy. Photons interact in materials almost exclusively with electrons surrounding the atom or by pair production in the field of the nucleus. The probability for an interaction depends on the atomic number of the material. Neutrons interact with atomic nuclei in a more complicated way.

An additional source of radiation is due to charged hadrons (e.g. protons, pions). However, the probability for producing hadron radiation is relatively low, and thus will be neglected here. The shielding is, nevertheless, effective for charged hadrons. The front wall will, for instance, stop 1 GeV protons.

The optimum shielding against radiation requires knowledge of the attenuation characteristics of the shielding material. The most common material for shielding against the types of

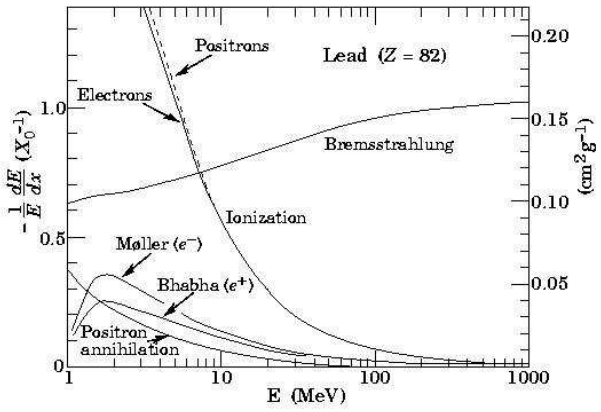

FIG. 2: *Interactions of electrons in lead. The energy loss is dominated by radiation (bremsstrahlung). Figure from [2]*

radiation discussed above is concrete, which may be composed of various materials of different densities. Typical concrete mixtures consist of 80% oxygen and silicon by weight, with the remainder comprised of calcium, aluminum, and to a lesser extend iron and potassium. The important component for neutron attenuation is hydrogen, which contributes less than 1% by weight in most concrete mixtures, but represents a significant fraction of the atoms in the material. Ordinary concrete has a density of 2.4 g/cm^3 [3]. The attenuation characteristics may vary slightly with composition. Sometimes, concrete is combined with higher density aggregates to increase its attenuation for photons and to reduce the space needed for shielding.

The existing shield house configuration for the HMS is composed of 100cm thick concrete lateral walls, 100cm concrete roof, and 100cm thick concrete secondary walls. In the front region, the outer wall is 200cm thick. The interior of the shield house is lined with a 5cm lead layer. The distance from the target to the inside of the lateral wall is 19.92m at an elevation of about 7m from the floor. Further details on the HMS shield house configuration can be found in the appendix.

The proposed design for the SHMS shield house is similar to the HMS design, but has several new features due to additional requirements. Figure 1 shows a schematic of the proposed design. The space between the beam side shield wall and the beam pipe is limited at very forward angles, and in addition, the length of the SHMS detector stack and minimum distance between the back of the detector hut to the hall wall require an evaluation of methods to reduce the thickness of the concrete shield wall. An important consideration is the effect of the radiation environment on the electronics for the detectors considered for the SHMS. It has been shown that many new commercial off the shelf components are more sensitive to radiation damage and single event upsets, requiring a careful evaluation of the impact of the radiation-induced effects on their performance and reliability [4].

Typical beam-target geometries were simulated using Monte Carlo techniques. Simulations

Concrete Thickness (cm)	Attenuation (no Boron)	Attenuation (add 1cm Boron)
50	2.42E-03	6.60E-06
100	2.79E-06	1.19E-08

TABLE I: *The attenuation of an incident 1 MeV neutron flux as calculated using the MCNP code [6]. MCNP suggests that 100 cm of concrete fully thermalizes 1 MeV neutrons. All remaining neutrons are captured by an additional boron layer.*

were performed using the GEANT MCWORKS distribution [5], which includes detailed physical and geometric descriptions of the experimental hall and simulates the physics processes using standard GEANT3 together with the DINREG nuclear fragmentation package. Hadronic interactions are treated using the DINREG package, which calculates the probability of such interactions using a database of photonuclear cross sections. For electron-nucleus interactions an "equivalent photon" representation of the electron (or positron) is used.

In this simulation, the CEBAF beam electrons start 1 m upstream of the target, strike it head-on along the cylindrical symmetry axis, and have no momentum component transverse to the beamline. The simulation also includes the beam pipe, target entrance and exit windows, and the entire geometry of Hall C, including all elements of the beam dump. The transmission of particles through the shielding materials was calculated as a function of the material thickness and the angle relative to the beam direction. Calculations were done simultaneously for the HMS and SHMS, and the background flux in the SHMS was normalized to the background flux in the HMS at 20°. This HMS angle provides a configuration that is known to keep radiation damage to the electronics at a reasonable level.

A limitation of the radiation studies is the lack of cross section data for low-energy neutrons. The accuracy of the GEANT simulations was tested by benchmark calculations using the MCNP code [6] with an isotropic neutron point source of 1 MeV located 1 m from the shield wall. The MCNP calculations suggest that 50cm of concrete thermalizes most of the fast neutrons, and after 1 m practically no epithermal neutrons remain (see Table I). The thermalized neutrons can be captured by a 1cm Boron layer. In reality, however, the neutron spectrum also includes higher energy neutrons, for instance produced by electrons interacting in the concrete, and thus the actual amount of material for the walls exposed to the primary sources of radiation has to be thicker. A simple transmission calculation using GEANT4 for incident neutron beams of energies between 1 and 10 MeV suggests that a thickness 150cm of concrete is sufficient to stop the majority of low-energy neutrons [7].

Material	X_0 (g/cm^2)	X (cm)
Air	36.20	30050
Concrete	23.0	9.2
Lead	6.37	0.56

TABLE II: *Radiation lengths for selected materials.*

II. ATTENUATING MATERIALS

The dominant interaction mechanism for electrons is energy loss through radiation, which produces photons. The effective material thickness for scattered electrons is thus expressed in terms of the radiation length, which denotes the distance over which the electron energy is suppressed by $1/e$. Table II lists the radiation lengths for common shielding materials. 200 cm of concrete (=20 X_0) stops scattered electrons. A lead layer placed after the concrete, an additional 10 X_0 absorbs the produced photons. The optimal shielding configuration thus consists of an attenuation material followed by a material with photon absorbing properties.

The effect of the material thickness on the penetrating power of photons and neutrons is quantified by the linear attenuation coefficients for each material.

$$I(x) = I_0 e^{-\mu x}, \tag{1}$$

where $\mu = \frac{N_A \rho}{A} = \frac{1}{\lambda}$ is the probability per unit length for the interaction.

Photons interact with matter through three mechanisms: the photoelectric effect, pair production, and Compton scattering. The likelihood of each of these processes depends on the energy of the photon as shown in Figure 3. In the case of the photoelectric effect, the photon is completely absorbed by an atom, which emits a photoelectron from a bound shell. The electron energy is equal to the energy of the photon minus the binding energy. The probability of the photoelectric effect increases with the atomic number (Z) of the material, as Z^4 or Z^5[8]. The effect is less likely to occur as the energy of the photon increases. Compton scattering involves a collision between a photon and an electron in which the photon transfers some of its energy to the latter. The energy of the outgoing photon depends on the angle. The Compton effect also depends on Z, and the photon energy, but to a lesser extent than the photoelectric effect. Pair production is the spontaneous creation of matter from energy. In close proximity to a nucleus, which absorbs part of the momentum, an energetic γ ray creates a positron-electron pair. Each particle requires 511 keV for formation, placing a lower limit of 1.022 MeV on the incident photon. Any photon energy $>$ 1.022 MeV goes into the kinetic energy of the pair. The probability of this occurring increases rapidly with higher photon energies. Overall, the best standard material for attenuating low-energy photons is lead.

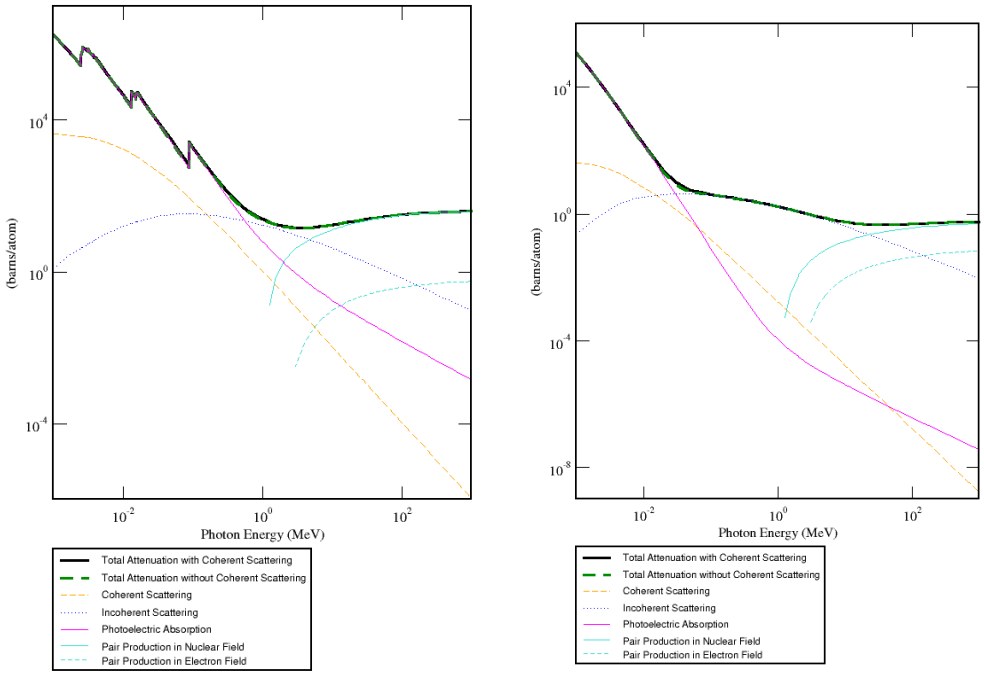

(a) *Cross section of photons in lead.* (b) *Cross section of photons in oxygen.*

FIG. 3: *The photon cross section in lead and oxygen. The total cross section is small at energies of 1-2 MeV. At low energies, the photoelectric effect dominates and absorption of photons is relatively easy. Pair production dominates at higher energies. The first step in designing shielding from photons is to attenuate photons from the difficult 1-2 MeV region. An effective shielding design is thus concrete followed by a high Z material (e.g. lead) to attenuate photons absorbing the low energy ones. Figure generated using the NIST XCOM database [9].*

Material	Z	μ (100keV) (cm^2/g)	μ (1 MeV) (cm^2/g)
Hydrogen	1	0.29	0.13
Iron	26	0.37	0.06
Tungsten	74	4.44	0.06
Lead	82	5.55	0.16

TABLE III: *Linear attenuation coefficients. Photon interact primarily with the electrons in the material, and thus high Z materials are most suitable to absorb low energy photons [9].*

The interaction of neutrons employs different mechanisms than the one for photons. Since the photon mainly interacts with the electrons surrounding an atom, the likelihood of γ interactions depends on the atomic number of the material. In contrast, neutron interactions depend on the nuclear properties. Different isotopes of the same element can have very different cross sections. For instance, odd-N nuclei will have larger capture cross sections than even ones. In general,

however, cross sections are larger at lower energies. For neutrons of energies higher than thermal (see table IV for energy ranges), it is thus very beneficial to first thermalize or slow down the fast neutrons. This is typically done through elastic scattering with hydrogen-rich materials such as concrete. Light elements are preferable since the energy loss per elastic collision is large in the lab frame. Thermal neutron (energies of 0.025 eV) can easily be captured. The capture cross section is particularly high for some elements such as boron [10], where the most relevant capture reaction channels are (n, γ), which has a small cross section and produces high energy photons [11], and (n, α), i.e.,

$$n + {}^{10}B \rightarrow {}^{7}Li + \alpha + \gamma[0.48MeV]. \tag{2}$$

This has a 94% probability to produce a 0.48 MeV γ ray from the excited ^{7}Li nucleus for each captured neutron [12]. The optimal shielding configuration thus contains a high Z material after the thermal neutron capturing material to absorb the produced capture photons. Photons may also be produced through neutron capture in the concrete, for instance on hydrogen, which turns into deuterium and emitts a prompt gamma ray of 2.2 MeV.

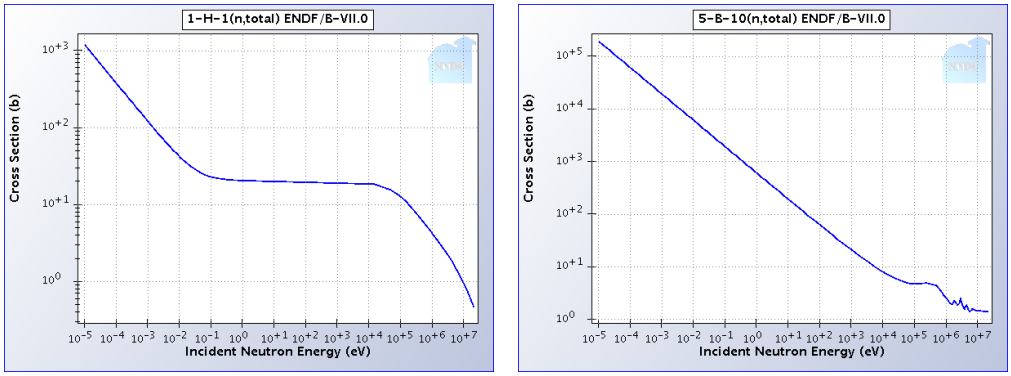

(a) *Cross section of neutrons in hyrogen.* (b) *Cross section of neutrons in boron.*

FIG. 4: *Cross section of neutrons in hydrogen and boron. The capture cross section is large only at very low energies. An important first step in shielding against neutrons is thus moderation. This involves slowing down fast neutrons through elastic scattering. This is typically accomplished with light elements, e.g. hydrogen, since the energy loss per collision is large. Figure generated using the neutrons NIST database [10].*

III. RESULTS

The SHMS shielding model is composed of standard concrete (ρ=2.4 g/cm^{-1}). The thickness of the walls in front of the detector and electronics huts is 200cm to shield from the primary radiation source around the target. Figure 5(a) shows the surviving background flux for varying front wall concrete thicknesses. The results are normalized to the background flux in the HMS at

Neutron Type	Energy Range
High Energy	>100 MeV
Fast	100 keV-10 MeV
epithermal	0.1eV-100 keV
thermal	0.025 eV

TABLE IV: *Classifications of neutron by their energy ranges.*

20°. This angle was chosen as recent experiments in Hall C have shown that electronics problems seem to dominate at lower angles [15]. The simulation results suggest that 200cm of concrete reduces the total flux to half of the HMS at 20°.

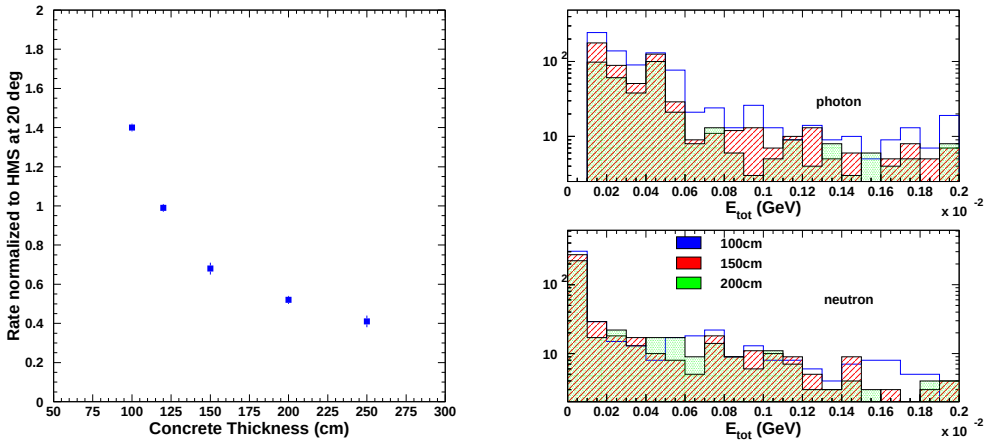

(a) *The normalized rate vs. front wall thickness. The rates are normalized to the HMS at 20°.*

(b) *The energy spectra for surviving photons and neutrons with varying front wall thickness.*

FIG. 5: *The Hall C GEANT simulation, which includes walls, roof, floor, and beam line components, suggests an optimal front shielding thickness of 2m. The right panel illustrates the outgoing particle spectrum, which is soft (< 10 MeV). For all rate calculations the spectrum.*

Figure 5(b) shows the energy spectra for surviving photons and neutrons with varying front wall thickness. In order to optimize the shielding, these secondary particles have to be absorbed as well. Our assumption on radiation damage is that photons below 100 keV will not be a significant source of dislocations in the lattice of the electronics components, while neutrons will cause radiation damage down to thermal energies. Adding lead to the concrete wall reduces the photon flux significantly, but it does not help for neutrons. On the other hand, the boron reduces the flux of very low energy neutrons. Assuming that low energy photons and neutrons cause a significant fraction of the radiation damage, then adding the relevant material would be important.

The thickness of the beamside wall (shielding from an extended source, the beamline) is

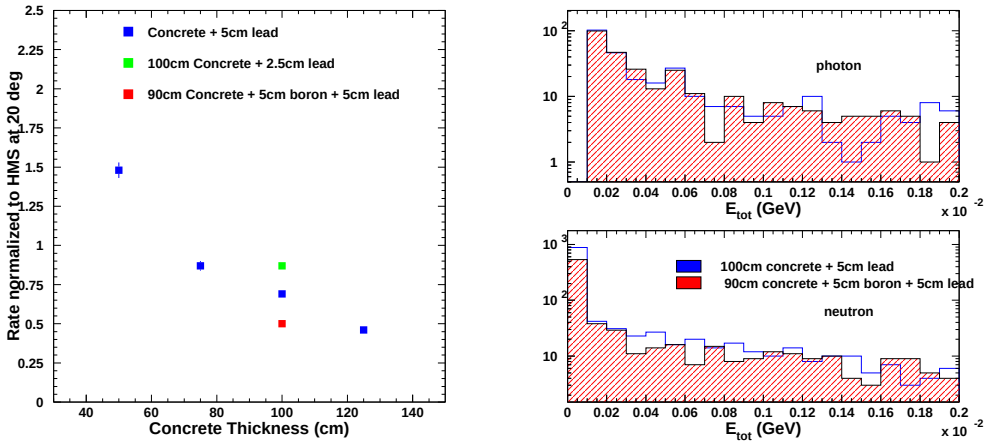

(a) *The normalized rate vs. the beamside conrete wall thickness.*

(b) *The energy spectra for surviving photons and neutrons with varying front wall thickness.*

FIG. 6: *The concrete shielding reduces the total background flux. Boron eliminates the thermal neutron background but produces 0.48 MeV capture photons. Adding lead reduces the low energy photon flux and absorbs capture photons. The total concrete thickness is limited due to space constraints.*

constrained by the clearance with the detector stack inside the hut and the beamline at small angles. Conservatively assuming a clearance of 5cm between detector stack and the shield wall, the total concrete wall thickness is limited to 105cm. A 90cm concrete wall combined with a 5cm boron and 5cm lead layer provides the optimal shielding configuration as illlustrated in Figure 6(a). Adding boron is not much different from adding (or replacing) concrete, but in addition it captures thermal neutrons.

The clearance between beamline and spectrometer shield wall requires that a section of the concrete wall be cut out. The cut section extends from the front to about 3/4 of the shield house length along the beam side (see Figure 7). The results from the simulation suggests that a cut of 30cm thickness at the front does not significantly contribute to the background rate. However, the background rate increases rapidly as the cut section increases.

The majority of charged particles is stopped by the outer walls of the spectrometer shield house. An additional source of radiation may be created from particles entering the detector hut through the magnets. In order to protect the electronics further, an intermediate wall will be installed between the detector and electronics hut. Figure 8 shows the normalized rate for varying concrete wall thickness. This suggests that the optimal configuration is provided by a concrete thickness of 80-100cm [17].

The walls not facing the main sources of radiation are used to shield from neutral particles scattered from the hall walls. The average energy spectrum of these particles is lower than the one for particles incident from the front. Figure 9 shows that a concrete wall thickness of 64cm is sufficient. Being exposed to a flux of neutrons of lower energies, the walls not facing the target

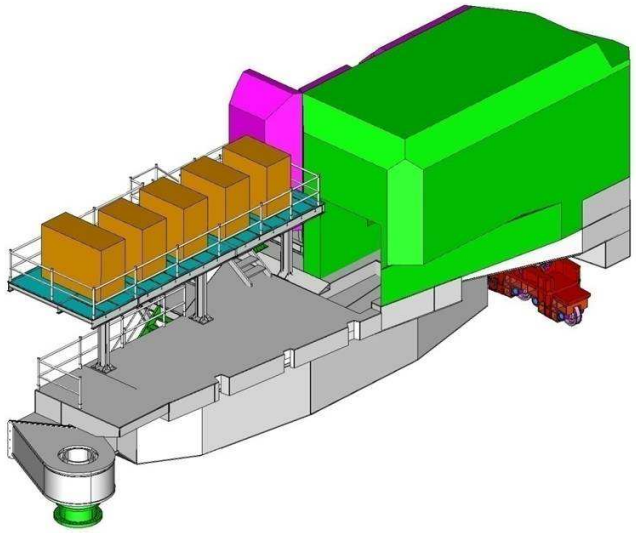

FIG. 7: *The close approach to the beamline at forward angles requires that a section be cut from the SHMS shield wall facing the beamline. The proposed cut section of 30 cm does not significantly contribute to the background flux. However, the background rate increases by a factor off about three as the cut out section increases.*

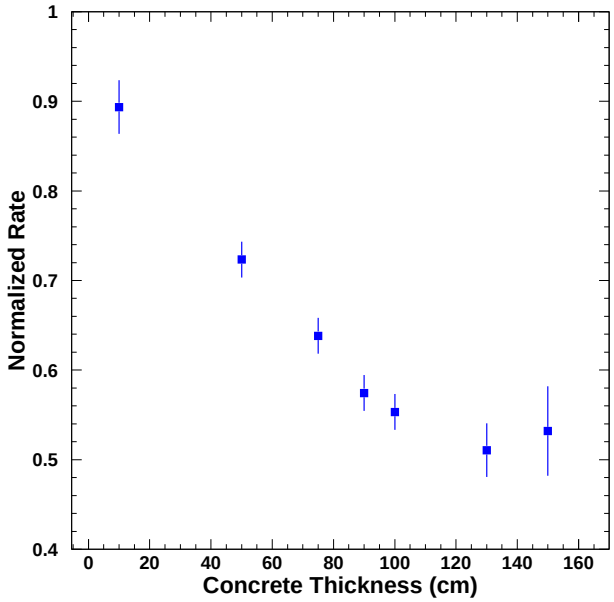

FIG. 8: *The normalized rate versus the intermediate concrete wall thickness.*

and beam line do not require equally extensive boron/lead shielding. However, at least 3mm of Boron and 5mm of Lead would be highly recommended to stop thermal and epithermal neutrons

and low-energy photons.

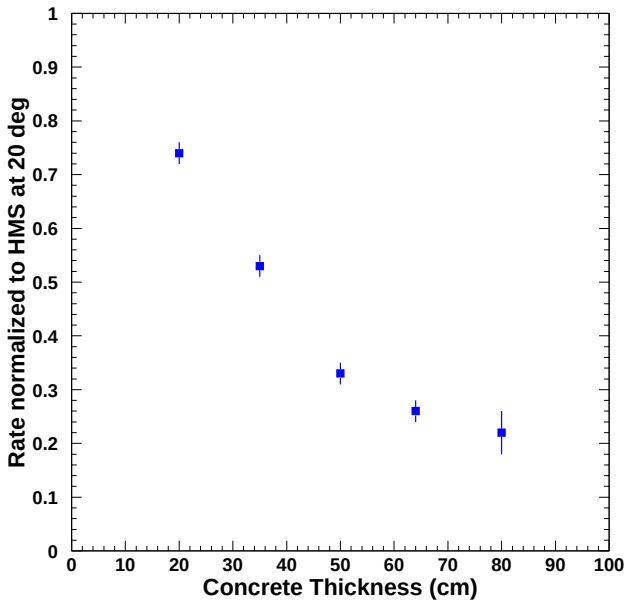

FIG. 9: *The normalized rate inside the spectrometer shield house for varying secondary wall thickness.*

The dimensions of the SHMS detector stack require a 172x172cm^2 window at the back of the SHMS detector hut. This opening is primarily exposed to radiation from the beam dump area. Monte Carlo simulations suggest that the SHMS rates at 20° are comparable to those for the HMS even without additional shielding. At forward angles, the SHMS rates are about a factor of two higher without the shielding.

Several available options for additional shielding were evaluated. The main options were: 1) addition of a thick concrete plug, 2) addition of a shield wall, and 3) addition of a shield wall and a thin plug. In all cases, the addition of shielding material has the largest effect at forward angles, while it has no significant effect for angles beyond 20°. Adding a thick concrete plug of 50cm provides an acceptable solution, but it limits the largest SHMS scattering angle to about 35° as the angular range of the spectrometer decreases by 5° for each addition of 50cm in thickness. Adding a concrete wall to shield from the beam dump provides an alternative solution, which does not interfere with the motion of the spectrometers. Both shielding options provide comparable background rates at forward angles. However, adding a thin concrete plug and a shield wall provides a more efficient shielding from low-energy background.

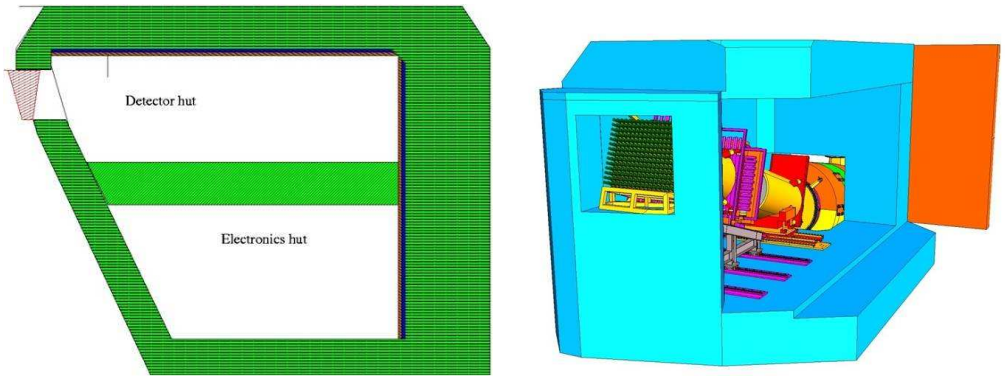

(a) (b)

FIG. 10: *The space requirement of the SHMS detector stack does not allow for a uniform back concrete wall design. In order to access the calorimeter PMTs for maintenance, a window is needed.*

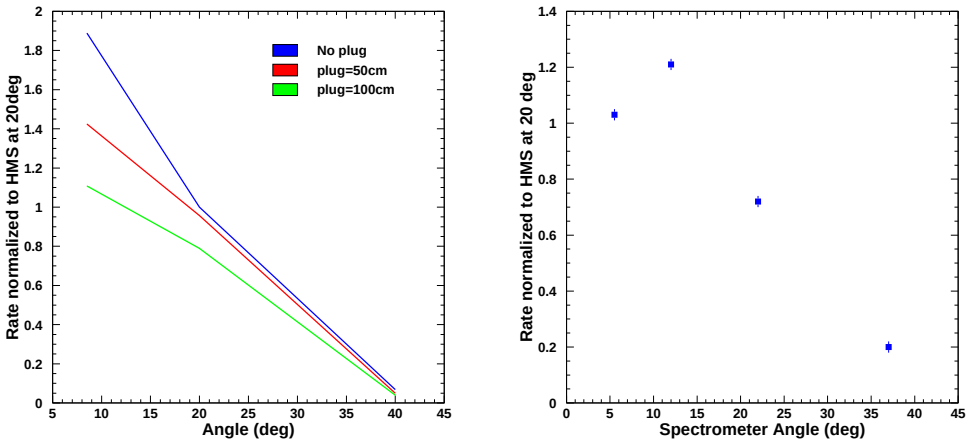

(a) *Concrete plug of uniform thickness.* (b) *Shield wall without plug.*

FIG. 11: *The angular distribution of the normalized background rate.*

IV. ORDERING OF SHIELDING MATERIALS

The hydrogen-rich concrete walls function as a shield, an absorber, and a neutron moderator, and are thus placed on the outside of all faces of the shield hut. On the other hand, the ordering of lead and boron to shield against the photon and neutron flux may, at first glance, not be obvious, and is discussed in detail below.

The incoming photon flux has two components: externally produced photons and bremsstrahlung photons produced by electrons in the twenty radiation lengths of concrete. The simulations have shown that the outgoing photon spectrum is soft (<10 MeV). Placing a lead layer after the concrete is essential to suppress this low energy photon flux. The (γ, n) reaction in lead is not a problem. The threshold for the reaction is given by the neutron binding energy ($\sim$ 8 MeV).

At higher energies, the cross sections are in the mbarn range [16]. Even disregarding the low cross section, however, it is not clear that this reaction adds to the radiating of the electronics, because a high energy photon is replaced by a low energy (but not thermal) neutron.

The incoming neutron flux also has two components. Neutrons from excited nuclei will typically not exceed 10 MeV. The other neutrons are produced through direct interactions with only one nucleon in the nucleus. These will have high energies, but the flux is low. As shown by the MCNP calculation, which has reliable low energy neutron cross sections, 0.5m of concrete almost fully thermalizes 1 MeV neutrons. Thus, 2m of concrete should be sufficient to thermalize the first component. Some of these will be captured in the concrete, but to eliminate the surviving thermal neutrons a layer of boron is needed. There are two relevant reaction channels: (n, γ) and $(n, \alpha\gamma)$. The former produces high energy photons, but the cross section is relatively small. The latter produces a 0.48 MeV photon for every captured neutron. The thermal cross section is about 10kbarn, and even at 1 MeV it is still in the barn range. The majority of neutrons can thus be expected to be captured in a sufficiently thick boron layer. An optimal shielding configuration would also stop these photons produced in the capture. At 0.48 MeV, the photoelectric effect and Compton scattering contribute about equally to the attenuation in lead. Photons from the latter will also need to be absorbed.

Thus, placing the lead in front of the boron layer has limited benefit. It will not affect the neutron flux, but will create an additional source of photons. The more lead one places after the boron, the more efficiently these photons will be suppressed. From the point of view of stopping bremsstrahlung photons, the order of boron and lead layers does not matter. Thus, all lead should be placed after the boron.

V. SENSITIVITY OF DETECTOR PMTS

During the G0 experiment a significant contribution of the background was found to be due to 0.48 MeV capture photons produced in the borosilicate glass window of the aerogel Cerenkov detector PMTs [12] through equation 2. The SHMS calorimeter phototubes will have the same borosilicate glass, which, at first glance, raises the issue of the calorimeter sensitivity to false readings due to the incident neutron flux.

However, the minimum ionizing peak for typical electrons and pions in the SHMS calorimeter is located at about 300 MeV, and so the calorimeter threshold is typically set to > 10 MeV. In contrast, the maximum energy deposited by photons produced from thermal neutron capture is 0.5 MeV, and thus negligible.

If a photon interacts directly in the photocathode, it will typically give one photoelectron, the smallest possible signal a photomultiplier tube can give,altough recent measurements have shown 1-4 photoelectrons contributing to the signal for borosilicate PMTs with 100KHz incident rates [12]. The SHMS GEANT simulation suggests a total photon flux into each calorimeter

detector element is about 0.1 MHz. Single pile ups within 10ns, which would affect the peak voltage, become significant for rates much larger than 10 MHz, and a pile up of 20 is rare even then.

The calorimeter is thus not sensitive to boron in the PMT windows. Additional boron lining preceeding a thin lead layer can be added to the back wall to provide shielding.

VI. CONCRETE DENSITY OPTIMIZATION

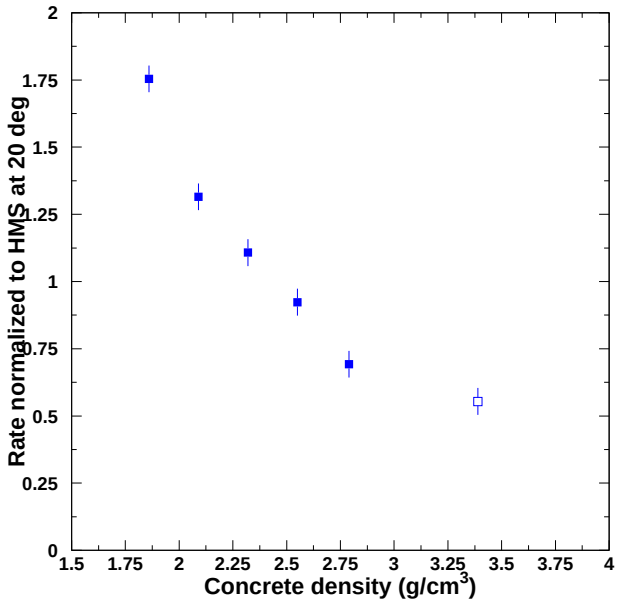

FIG. 12: *The dependence of the normalized SHMS rate on the concrete density. The open symbol denotes the rate calculated with the iron content in the concrete replaced with tungsten.*

The addition of high density aggregates can increase its attenuation for photons and reduce the space needed for shielding. Figure 12 summarizes the effect of increasing the density from its nominal value assuming that concrete is compressible. While increasing the density reduces the background flux, the total effect is limited to a factor of about two. In addition, the search for aggregates is limited to silicone oxide based materials (e.g. granite), and since more than 80% of ordinary concrete already consist of sand, adding more may affect the structural soundness of the shield house. The optimal solution for optimizing the shield house concrete composition would be to increase the hydrogen content as this would improve the shielding against neutrons.

VII. SUMMARY

The radiation environment is an important consideration for the design of the SHMS shield house, in particular, the effect of radiation-induced effects on the performance and reliability of detectors and electronics. The SHMS shield hut wall thicknesses have been optimized to provide proper shielding for the detectors. The separate electronics hut provides for even better radiation shielding. The SHMS shielding configuration includes concrete walls to moderate and attenuate particles. Low energy (thermal) neutrons are absorbed in a boron layer. Low energy and 0.5 MeV capture photons are absorbed in lead. With the proposed SHMS shield hut design, the rates at forward angles of 5.5° are estimated to be 70% of the design goal (HMS at 20°) in the detector hut and $< 50\%$ in the electronics hut.

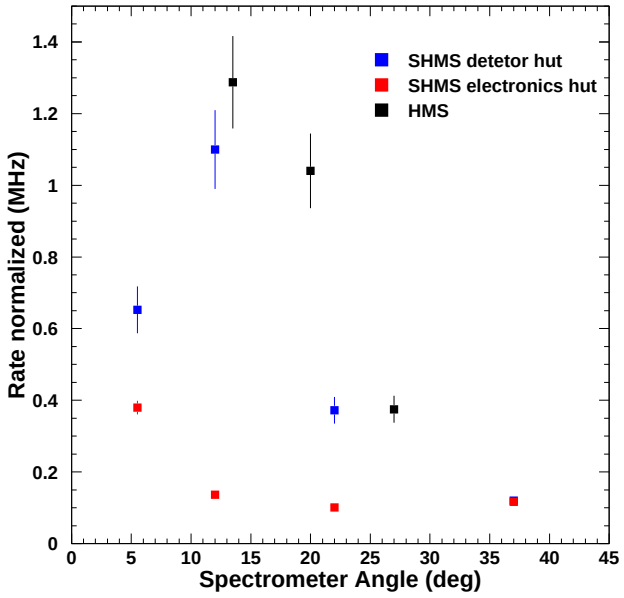

FIG. 13: *The dependence of the SHMS and HMS rates on the spectrometer angle.*

VIII. ACKNOWLEDGEMENTS

We thank P. Degtiarenko for providing a general version of the MCWORKS code and some other people for helpful discussions.

[1] W. R. Leo, *Techniques for Nuclear and Particle Physics Experiments*, second edition, Springer Verlag Berlin, Heidelberg 1987, 1994

[2] C. Caso *et al.*, The European Physical Journal **C3** (1998) 1.

[3] Portland Cement Association, .

[4] P. J. Griffin *et al.*, *The role of thermal and fission neutrons in reactor neutron-induced upsets in commercial SRAMSs*, IEEE NS Vol. 44, No. 6, Dec. 1997.

[5] P. Degtiarenko, private communication.

[6] J. F. Briesmeister (ed.), MCNP - A General Monte Carlo N-particle Transport Code Version A, LA-12625-M, Los Alamos National Laboratory, Los Alamos, New Mexico (1993).

[7] S. Wood, private communication (2008).

[8] J. R. Lamarsh, Introduction to Nuclear Engineering 2nd ed., Addison-Wesley, (1983)

[9] M. J. Berger *et al.*, XCOM: Photon Cross Sections Database, NIST Standard Reference Database 8 (XGAM), 1998. *http://physics.nist.gov/PhysRefData/Elements/per_noframes.html*

[10] Neutron News, Vol. 3, No. 3, 1992, 29-37. *http://www.ncnr.nist.gov/resources/n-lengths/*

[11] M. D. Goldberg *et al.*, Neutron Cross Sections, Sigma Center, Brookhaven National Laboratory (1966), *http://www.nndc.bnl.gov/sigma/index.jsp*

[12] H. Breuer *et al.*, *Neutron detection studies in bare photon tubes using cold neutrons at NIST*, UMD Technical Report Number: PP# 06-052 (2006).

[13] C. I. Underwood, *The Single-Event-Effect Behaviour of Commercial-Off-The-Shelf Memory Devices - A Decade in the Low-Earth orbit*, IEEE Transactions on Nuclear Science Vol. 45, No. 3, June 1998.

[14] G. R. Srinivasan, *Parameter-free predictive modeling of single event upsets due to protons, neutrons and pions in terrestial cosmic rays*, IEEE Transactions on Nuclear Science Vol. 41, No. 6, Dec. 1994.

[15] M. Jones *et al.*, private communication (2008).

[16] Birenbaum *et al.*, Phys. Rev. **C51**, (1995) 3496

[17] Note that a minimum wall thickness of 50cm is needed for the construction of the roof of the shield house

IX. APPENDIX: HMS SHIELDING

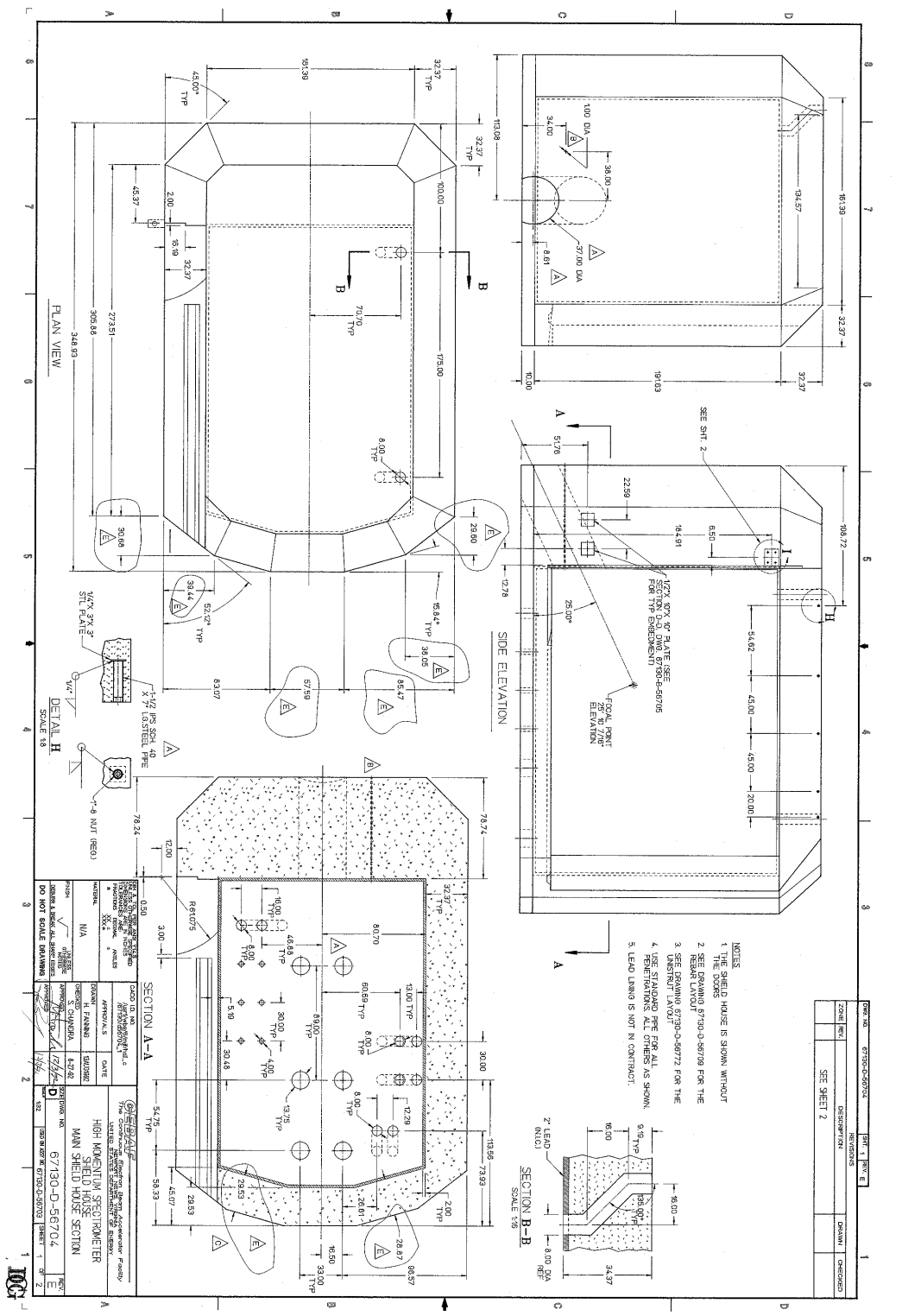

FIG. 14: *HMS shield house drawing E-67130-56704 (part 1).*

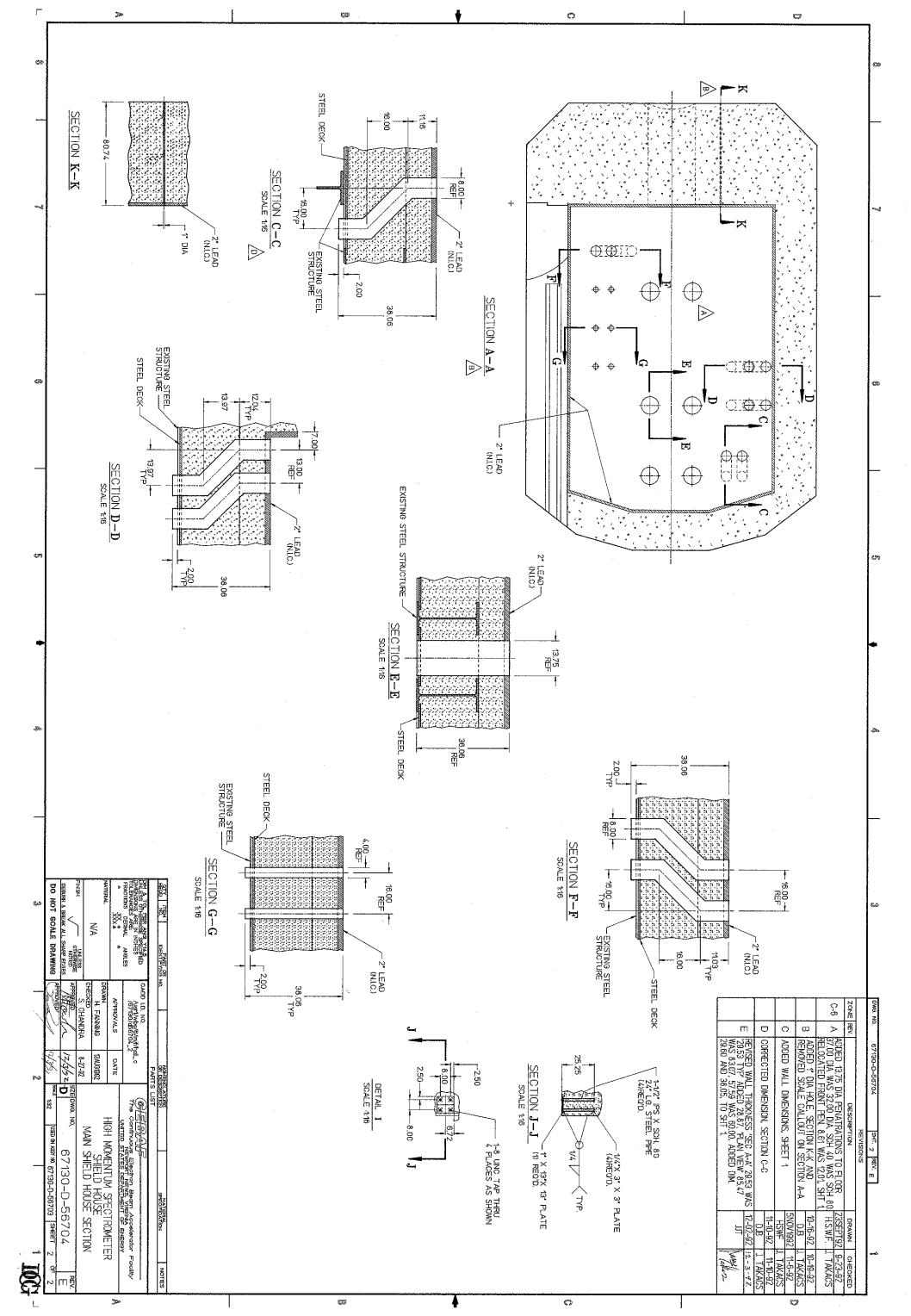

FIG. 15: *HMS shield house drawing E-67130-56704 (part 2).*

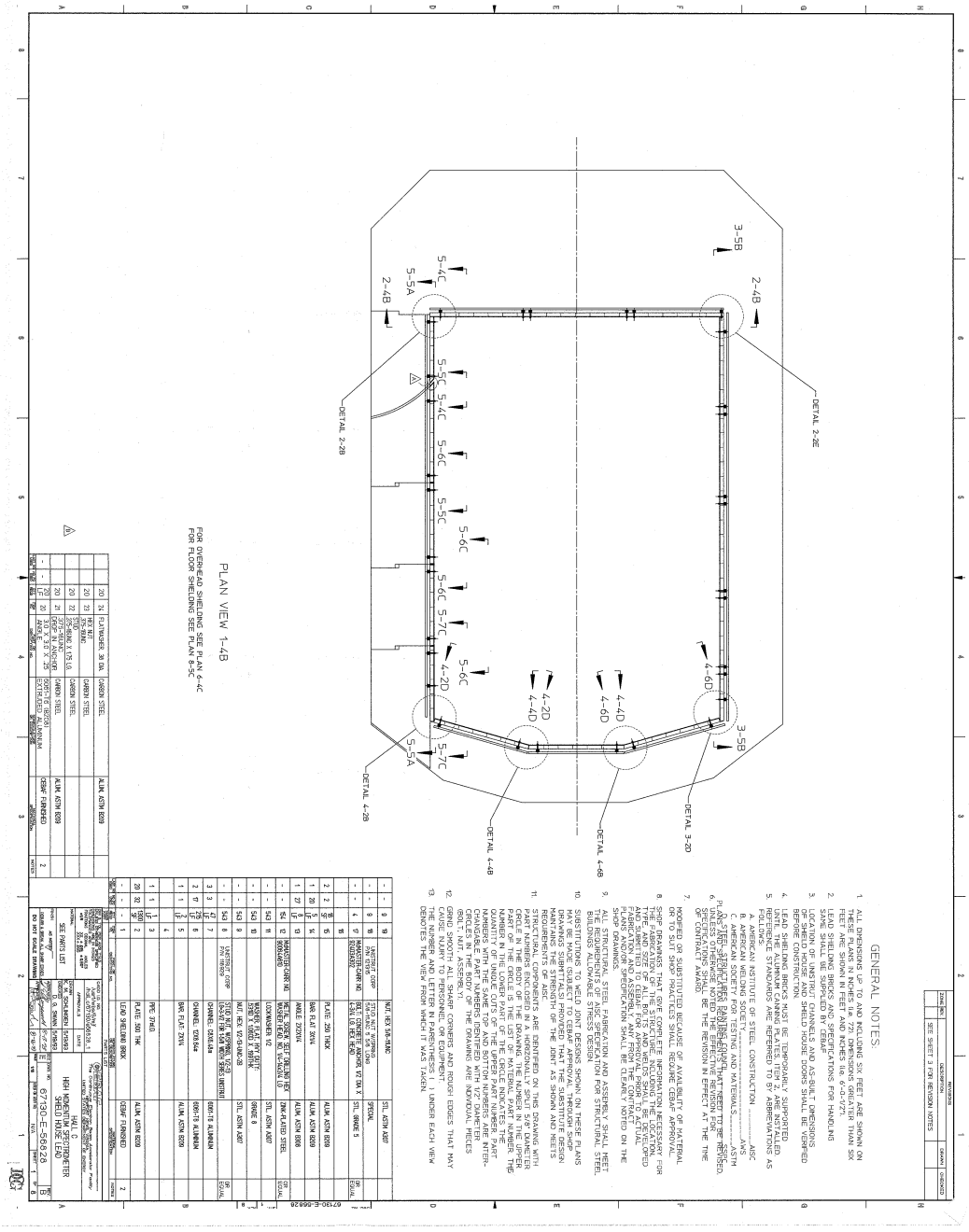

FIG. 16: *HMS shield house drawing E-67130-56828.*

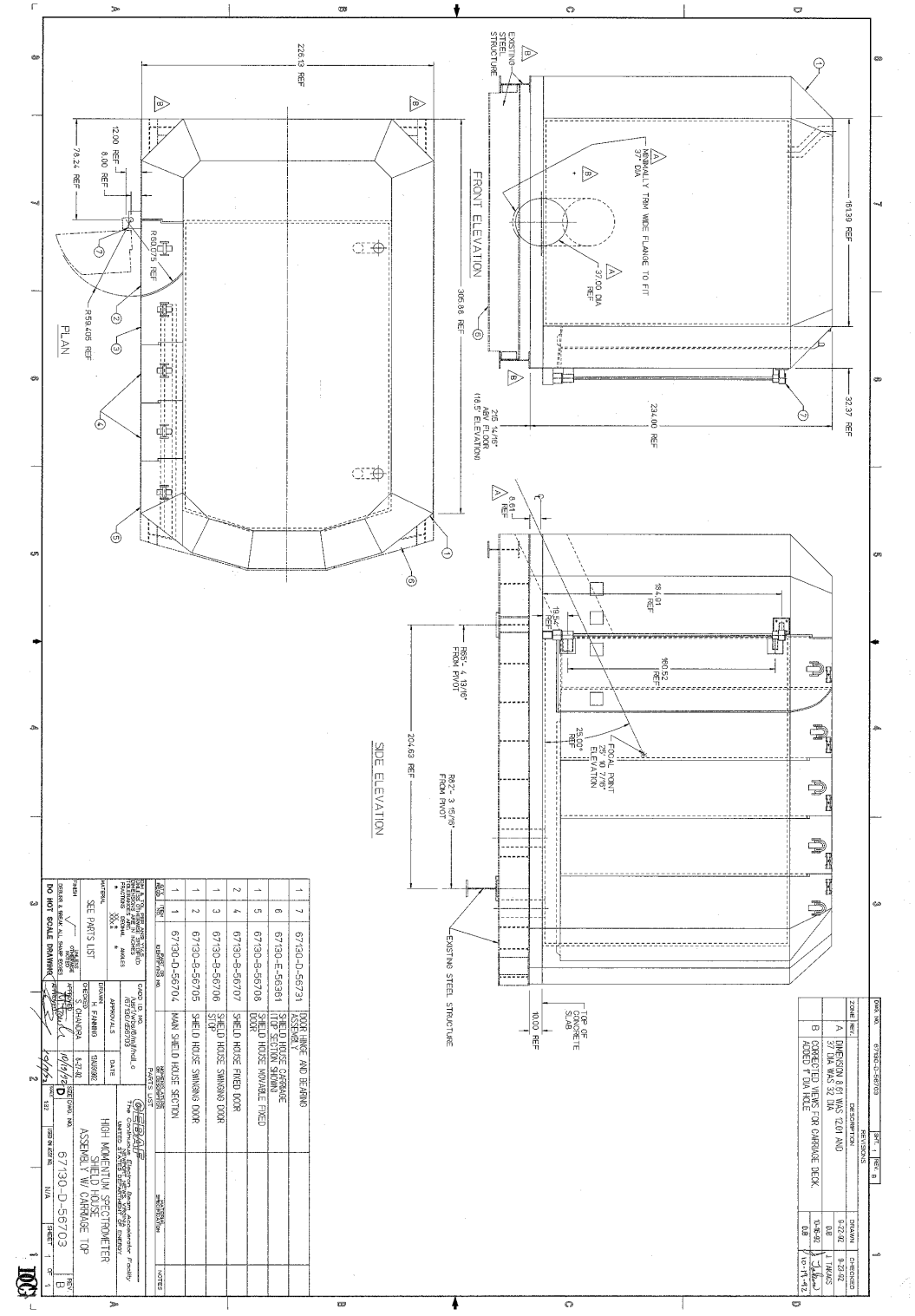

FIG. 17: *HMS shield house drawing E-67130-56703.*